iop

by Salnid Basir

Submission date: 21-May-2023 01:15PM (UTC+0700)
Submission ID: 2098136223
File name: Salni_2021_IOP_Conf._Ser.__Earth_Environ._Sci._926_012050.pdf (1.02M)
Word count: 3171
Character count: 15972

PAPER · OPEN ACCESS

Solution combustion method to synthesize magnetic Fe_3O_4 as photocatalytic of Congo red dye and antibacterial activity

To cite this article: Salni *et al* 2021 *IOP Conf. Ser.: Earth Environ. Sci.* **926** 012050

Solution combustion method to synthesize magnetic Fe_3O_4 as photocatalytic of Congo red dye and antibacterial activity

Salni[1], M Said[2], P L Hariani[2*], I Apriani[3]

[1]Department of Biology, Faculty of Mathematics and Natural Sciences, Universitas Sriwijaya, Jalan Palembang-Prabumulih, Indralaya, Indonesia
[2]Department of Chemistry, Faculty of Mathematics and Natural Sciences, Universitas Sriwijaya, Jalan Palembang-Prabumulih, Indralaya, Indonesia
[3]Doctoral Program, Faculty of Mathematics and Natural Sciences, Universitas Sriwijaya, Jalan Palembang-Prabumulih, Indralaya, Indonesia

*Email: puji_lukitowati@mipa.unsri.ac.id

Abstract. Fe_3O_4 has been synthesized using the combustion solution method using glycine as fuel. The Fe_3O_4 was used as a catalyst in the photocatalytic degradation of Congo red dye. The Fe_3O_4 were characterized using X-ray diffraction (XRD), scanning electron microscopy (SEM), and energy-dispersive X-ray spectroscopy (EDS), UV-Vis spectroscopy, and vibrating sample magnetometry (VSM). The characterization showed that Fe_3O_4 has an inverse spinel structure with a crystalline size of 35.6 nm. Fe_3O_4 has an optical band gap of 2.16 eV, and a saturation magnetization of 83.76 emu/g. The study showed that the highest photocatalytic degradation was at 90 min of irradiation time using visible light irradiation, the concentration of Congo red dye of 10 mg/L, and pH solution of 5, with a photocatalytic degradation efficiency of 97.70%. The experiment indicated that the photocatalytic degradation of the Congo red dye by Fe_3O_4 followed a pseudo-first-order. Fe_3O_4 is effective as an antibacterial against gram-positive bacteria (*Streptococcus aureus*) and gram-negative bacteria (*Escherichia coli)*.

1. Introduction

In recent years, research on nanomagnets has received intensive attention in the engineering and medical fields. Materials in nanoscale have unique physical, chemical, and biological properties, compared to those in large sizes [1]. Spinel ferrites are compounds with the general formula MFe_2O_4, where M is a cation like Mn, Fe, Co, Ini, Zn, etc [2]. Fe_3O_4 (magnetite) serves as one of the important ferrites due to its small size, large magnetic properties, biocompatibility and biodegradability, and low toxicity [3,4]. It has many functions, such as in the biomedical field, namely as an antibacterial and antioxidant agent, catalyzation, drug delivery, adsorption, magnetic recording media, and lithium-ion battery [1,3,4,5,6].

Heterogeneous photocatalysis is considered an attractive method because it has been successfully used for degrading various organic pollutants. The increasing use of photocatalytic methods, compared to conventional methods, is due to its capability of degrading organic substances into harmless molecules such as CO_2, H_2O, and organic acids [7]. Fe_3O_4 has been used as a photocatalyst to degrade Methylene blue, Congo red, Methyl orange, Rhodamine B, and Levofloxacin dyes [1,8,9]. The increase in the photodegradation efficiency of organic molecules in the visible-magnetic Fe_3O_4 irradiation system can be attributed to the fast electron transfer resulting in effective electron and hole separation. A hole is a strong oxidizing agent that can oxidize OH and H_2O adsorbed on the Fe_3O_4 surface, producing H_2O

free radicals. The H_2O radicals adsorbed on the Fe_3O_4 surface are strong oxidants that oxidize the adsorbed organic compounds. The superparamagnetic properties of Fe_3O_4 increase the efficiency of separating the catalyst from the solution after the degradation process. In a short time, the separation can be done using a permanent magnet.

Fe_3O_4 can be synthesized by various methods, including co-precipitation [3], sol-gel [10], hydrothermal [11], solvothermal [12], and solution combustion [13]. The solution combustion method has a simple procedure with a short reaction time and high purity product [14]. The organic compounds used in the solution combustion method as fuel are urea, glycine, EDTA, and citric acid [15]. The type of fuel used affects the intensity of the combustion reaction [16]. The synthesis of $NiFe_2O_4$ shows that glycine as fuel has greater crystallinity than urea and citric acid [17].

In this study, Fe_3O_4 was synthesized using glycine as fuel by the solution combustion method. Next, Fe_3O_4 was employed to degrade Congo red dye with visible light irradiation. Congo red dye is a benzidine-based anionic dye that is soluble in water and challenging to decompose due to its structural stability. It is widely used in the textile, tanning, printing, dyeing, paper, rubber, and plastics industries [18,19,20]. The antibacterial properties of Fe_3O_4 were tested against bacteria commonly found in wastewater, namely *S. aureus* and *E. coli*.

2. Materials and Methods

The materials used in this study were $Fe(NO_3)_3.9H_2O$, $C_2H_5NO_2$, Congo red of Sigma Aldrich company, and bacteria species of *S. aureus* ATTC 25923 and *E. coli* ATCC 25922 from PT Bio Farma.

2.1. Synthesis of Fe_3O_4

$Fe(NO_3)_3.9H_2O$ and $C_2H_5NO_2$ were dissolved in deionized water, then the mixture was stirred until homogeneous. The mixture was then poured into a round bottom flask with a perforated rubber stopper to release the reaction gas. The mixture was heated on a hot plate at controlled temperatures. Heating was continued gradually until reaching a particular temperature to form a gel. In the next few minutes, a violent reaction occurred while releasing gas and leaving Fe_3O_4 powder, which was then ground with a mortar. The reaction occurring was [21]:

$$54Fe(NO_3)_3 + 92C_2H_5NO_2 \rightarrow 18\,Fe_3O_4 + 184CO_2 + 230H_2O + 127N_2$$

The resulting Fe_3O_4 was characterized using X-ray diffraction (XRD Malvern Panalytical) to obtain crystal structure and crystalline size. XRD analysis was done on CuKα irradiation (λ = 1.5406Å), with a range of 2θ = 20-90°. The magnetic properties of Fe_3O_4 were analyzed using a vibrating sample magnetometer (VSM Oxford Type 1.2 T). The morphology and elemental composition were analyzed using a scanning electron microscope–energy dispersive spectrometer (SEM-EDS JOEL JSM 6510 LA). The optical absorption spectra were determined using UV-visible diffuse reflectance spectroscopy (UV-Vis DRS Pharmaspec UV-1700).

2.2. Photocatalytic Degradation

Photocatalytic degradation of Fe_3O_4 against Congo red dye occurred by irradiation of visible light (λ=420 nm). For the time variable, a total of 10 mg of magnetic Fe_3O_4 was put into 25 mL of Congo red 20 mg/L dye solution then stirred using a magnetic stirrer. The irradiation time was varied between 10-100 minutes with 10 minutes difference. For the concentration variable, the concentration of Congo red was varied in the range of 10-80 mg/L. Meanwhile, for the pH variable, the pH of the solution was varied with the range of 3-9. The remaining undegraded Congo red dye concentration was analyzed using a UV-Vis spectrophotometer (Type Orion Aquamate 8000).

2.3. Testing the antibacterial activity

The antibacterial activity test was carried out using the agar well diffusion method. A total of 500 µL of bacterial cultures (*S. aureus* and *E. coli*) were put onto a Petri dish containing nutrient agar. After

the media was solidified, holes were made, and Fe_3O_4 was put into them with different concentrations ranging from 2[illegible]o 125 g/mL. The Petri dish was wrapped with parafilm tape and transferred to an incubator to be incubated at 37°C for 24 hours. The diameters of the clear zones formed were measured in millimeters.

3. Results and Discussion

3.1. *Characterization of Fe_3O_4*

Figure 1(a) shows the XRD spectra of Fe_3O_4. The crystalline peaks of Fe_3O_4 can be observed at 2θ, namely, 30.25°, 35.71°, 43.35°, 53.73°, 57.35°, and 62.85°, corresponding to the planes (220), (311), (400), (422), (511), and (440), (531) and (533). The 2θ angle confirmed JCPDF file No. 89-0691, namely Fe_3O_4 inverse spinel structure. The crystalline size of Fe_3O_4 obtained an average of 35.6 nm. The crystalline size of Fe_3O_4 was smaller than in other studies synthesizing by co-precipitation method, which is ~40 nm [22].

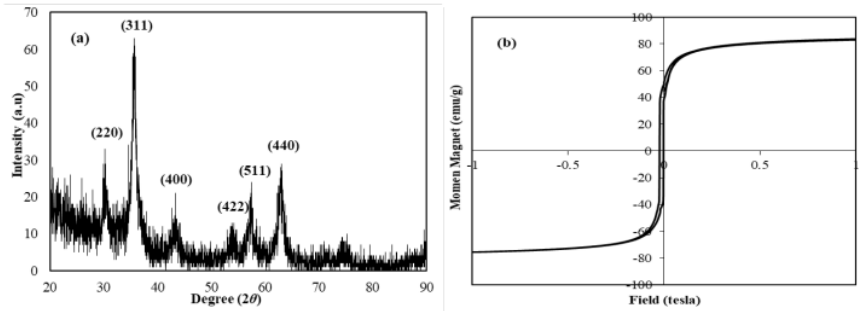

Figure 1. (a) XRD spectra and (b) magnetic hysteresis loop of Fe_3O_4

The magnetic properties of Fe_3O_4 determined using VSM are present in Figure 1(b). The specific saturation magnetization value of Fe_3O_4 was obtained at 83.76 emu/g, higher than the Fe_3O_4 synthesized using the co-precipitation method, which is 74.33 emu/g [3], and the thermal decomposition method is 67 emu/g [23]. A great saturation magnetization value indicates superparamagnetic properties.

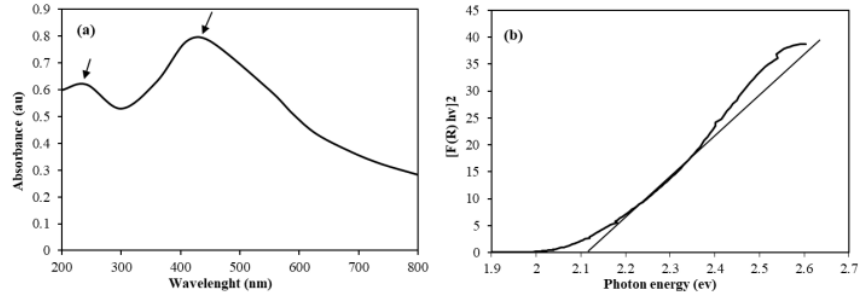

Figure 2. (a) UV-Vis spectra and (b) optical band gab of Fe_3O_4

The optical absorption spectra of Fe_3O_4 are shown in Figure 2a. The results of UV-Vis absorption confirmed that Fe_3O_4 produced more electrons in the visible light region, where the optimum peak was at 443 nm. If the incident light energy equals the photocatalyst band gab energy, electrons will be excited from the valence band to the photocatalyst conduction band. Figure 2b shows Kulbeka Munk model on by linear extrapolation plot of $[F®hv]^2$ versus hv gives a band gap of 2.16 eV. The ferrite band gap is

about ~2.0 eV, effective for absorbing visible light [24]. The band gap is not much different from Fe_3O_4 synthesized by the co-precipitation method, which is 2.17 eV [22].

Figure 3(a) shows the morphology of Fe_3O_4 analyzed using SEM, while Figure 3(b) the EDS spectra of Fe_3O_4. The morphology of Fe_3O_4 appears to be spherical but not homogeneous. The small particle size causes Fe_3O_4 to agglomerate. Based on the EDS results, Fe_3O_4 contains 71.86% O and 28.14% Fe, with no other elements. Therefore, the Fe_3O_4 synthesized by the solution combustion method has high purity.

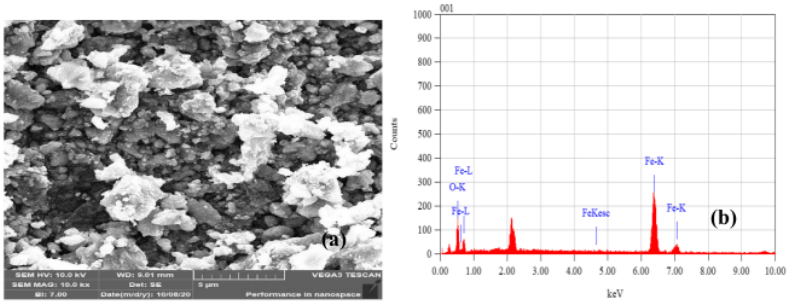

Figure 3. (a) SEM image dan EDS spectra of Fe_3O_4

3.2. Photocatalytic Activity of Fe_3O_4

The effect of irradiation time, Congo red dye concentration, and solution pH on photocatalytic degradation efficiency is shown in Figure 4. The optimum irradiation time was 90 minutes, at which the dye was degraded by 87.50%. The further addition of irradiation time showed that the amount of the dye degraded was relatively constant. The degradation found in this research was more than the photodegradation of Congo red dye using $CoFe_2O_4$, which is 84-92% [25]. In the presence of a visible light source, photons excited electrons on the surface of the catalyst (Fe_3O_4), where electrons moved from the valence band to the conduction band, leaving positive holes in the valence band, which then reacted with water to release hydroxyl ions, which degraded the dye [26].

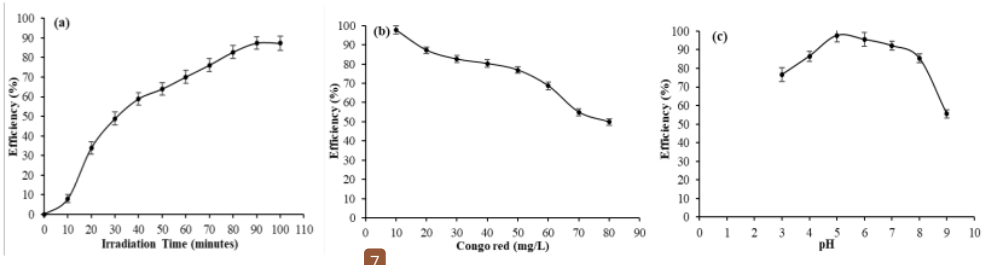

Figure 4. Photocatalytic degradation of Congo red dye; effect of (a) irradiation time, (b) concentration of Congo red dye, (c) pH solution

Figure 4 (b) shows that an increase in the concentration of Congo red dye caused a decrease in photocatalytic degradation efficiency. A high concentration of dye blocked the interaction between visible light with the catalyst's surface so that the degradation ability of the catalyst decreased. In addition, the number of hydroxyl radicals produced by the catalyst was limited while the amount of dye increased [25]. The same phenomenon in the photocatalytic degradation of Congo red dye using $CoFe_2O_4$ [26]. Figure 4(c) indicates that optimum efficiency was at pH 5, reaching 97.70%. There was a decrease in photodegradation efficiency when the pH increased. Fe_3O_4 has a pHpzc of 7-7.4 [27]. The Congo red dye is an anionic dye. At a pH greater than pHpzc, there is a repulsion between the negative

charge of the dye and the catalyst. At low pH, there is an attractive competition between the anionic dye and H^+ with the catalyst. In this study, the highest efficiency was at a pH of 5.

The pseudo-first-order kinetics was determined using the equation [26]:

$$ln\frac{C_o}{C_t} = kt$$

C_0 is the initial concentration of dye (mg/L), C_t is the concentration of the dye at a certain time (mg/L), t is time (min), and k is the velocity constant (min^{-1}). A pseudo-first-order kinetic model has been adopted to describe the dye photocatalytic degradation process using ferrites [28,29]. Figure 5 shows that the photocatalytic degradation process of Congo red dye follows a pseudo-first-order. The correlation coefficient (R^2) is 0.9969, the rate constant value (k) is 0.0308 min^{-1}, and the half-life time ($t_{1/2}$) is 22.5 min.

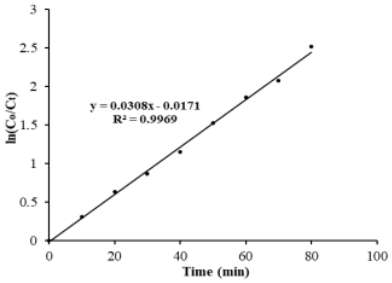

Figure 5. Pseudo-first-order kinetics of photocatalytic degradation Congo red dye by Fe_3O_4

3.3. *Antibacterial Activity of Fe_3O_4*

Fe_3O_4 is an effective antibacterial agent, as shown in Figure 6. Reactive oxygen species (ROS) produced by Fe_3O_4 causes oxidative stress of the bacteria. ROS include radicals such as superoxide radicals ($O_2^{\bullet}$), hydroxyl radicals ($^{\bullet}OH$), and hydrogen peroxide (H_2O_2), which are responsible for protein and DNA damage in bacteria [1,30]. ROS can be produced by iron oxides such as Fe_3O_4 that cause inhibition of most pathogenic bacteria. This study showed that the zone of inhibition of gram-positive bacteria is smaller than gram-negative bacteria. Gram-negative bacteria are more sensitive than gram-positive. Each bacterium has a distinctive cell structure and metabolic peculiarities [30,31].

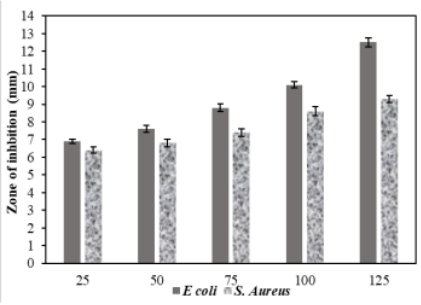

Figure 6. Antibacterial activity of Fe_3O_4 against *S. aureus* and *E. coli*

4. Conclusion

Fe_3O_4 has been successfully synthesized by the solution combustion method using glycine as fuel. Fe_3O_4 has a spinel structure with a crystal size of 35.6 nm and is superparamagnetic. Fe_3O_4 in combination

with visible light effectively in the photocatalytic degradation of Congo red dye. The photocatalytic degradation optimum process at 90 min of irradiation time, Congo red dye concentration of 10 mg/L, and a pH solution of 5 with the efficiency of 97.70%. Pseudo-first-order is appropriate to describe the photocatalytic degradation process of Congo red dye. Fe_3O_4 is effective as an antibacterial against gram-positive and gram-negative bacteria. Thus, Fe_3O_4 is preferable to be used for processing industrial wastewater, especially those containing synthetic dyes.

References

[1] Kumar B, Smita K, Cumbal L, Debut A, Galeas S, Guerrero V H 2016 *Mater. Chem. Phys*. **179** 310
[2] Amulya M A S, Nagaswara H P, Kumar M R A, Ravikumar C R, Prashantha S C, Kususma K B 2020 *Appl. Surf. Sci. Adv*. **1** 10023
[3] Hariani P L, Desnelli, Fatma, Putri R I, Salni 2018 *J. Pure App. Chem. Res*. **7** 122
[4] Zhang L, Dong W F, Sun H B 2013 *Nanoscale* **5** 7664
[5] Gao J H, Gu H W, Xu B 2009 *Acc. Chem. Res*. **42** 1097
[6] Yew Y P, Shameli K, Miyake M, Khairudin N B A, Mohamad S E, Naiki T, Lee K X 2020 *Arab. J. Chem*. **13** 2287
[7] Stylidi M, Kondarides D I, Verykios X E, 2003 Appl. *Catal. B Environ.* **40** 271
[8] Giri S K, Das N N, 2016 *Desalin.* **57** 900
[9] Hu J D, Zevi M, Kou X M, Xiao J, Wang X J, Jin Y 2010 *Sci. Total Environ.* **408** 3477
[10] Lemine O, Omri K, Zhang B, Mir E, Sajieddine M 2012 *Superlattices Microstruct*. **52** 793
[11] Haw C Y, Mohamed F, Chia C H, Radiman S, Zakaria S, Huang N M, Lim H N 2010 *Ceram. Inter*. **32** 1417
[12] Luo Y, Yang J, Yan Y, Li J, Shen M, Zhang G, Mignani S, Shi X 2015 *Nanoscale* **7** 14538
[13] Lesbayev A B, Smagulova G T, Kim S, Prikhod'ko N G, Mankov S M, Guselnov N, Mansurov Z A 2018 J. *Self-Propagating High-Temp. Synth.* **27** 195
[14] Lazarova T, Georgieva M, Tzankov D, Voykova D, Aleksandrov L, Zheleva Z C, Kovacheva D 2017 *J Alloys Comp.* **700** 272
[15] Nguyen L T T, Nguyen L T H, Manh N C, Quoc D N, Quang H N, Nguyen H T T, Nguyen D C, Bach L G 2019 *J. Chem.* **2019** 1
[16] Toniolo J, Takimi A, Andrade M J, Bonademan R, Bergman C P 2007 *J. Mater. Sci.* 42 4785
[17] Karakas Z K, Boncukeuogiu R, Karakas I H 2016 *J. Phys. Conf. Ser.* **707** 1
[18] Purkait M K, Maiti A, Dasgupta S 2007 *J. Hazard. Mater.* **145** 287
[19] Mittal A, Mittal J, Malviya A, Gupta V K 2009 *J Colloid Interface Sci.* **340** 16
[20] Ahmad R, Kumar R 2010 *Appl. Surf. Sci.* **257** 1628
[21] Wang X, Qin M, Fang F, Jia B, Wu H, Qu X, Volinsky A A 2017 *J. Alloy Comp.* **719** 288
[22] Reddy I N, Sreedhar A, Reddy C V, Shim J, Cho M, Kim D, Gwag J S, Yoo K 2018 *J. Solid State Electrochem.* **22** 3535
[23] Jia X, Chen X, Liu Y, Zhang B, Zhang H, Zhang Q, 2019 *Appl. Organometallic Chem*. **33** 1
[24] Casbeer E, Sharma V K, Li X Z 2012 *Sep. Purif. Technol.* **87** 1
[25] Ali N, Said, A, Ali F, Raziq F, Ali Z, Bilal M, Reinert L, Begum T, Igbal H M N 2020 Water Air Solut Pollut 231 1
[26] Vijay S, Balakrishnan R M, Rene E R Priyanka U 2019 *J. Water Supply Res. T*. **68** 666
[27] Rajput S, Pittman C U Jr, Mohan D 2015 *J. Colloid Interface Sci.* **468** 334
[28] Hariani P L, Said M, Rachmat A, Riyanti F, Pratiwi H C, Rizki W T 2021 *Bull. Chem. React. Eng. Catal.* **16** 481
[29] Loan N T T, Lan N T H, Han N T T, Hai N Q, Anh D T T, Hau V T, Tan L V, Tran T V 2019 *Processes* **7** 1
[30] Gabrielyan L, Hovhannnisyan A, Ananyan M, Trchounian A 2019 *Appl. Microbiol. Biotechnol.* **103** 2773
[31] Prabhu Y T, Rao K V, Kumari B S, Kumar V S S, Pavani T 2015 Int. Nano Lett. **5** 85

Acknowledgment
This research was supported by grant under the program of "Penelitian Dasar Unggulan Perguruan Tinggi ". Contract No. 0166.15/UN9/SB3.LP2M.Pt/2021.

iop

ORIGINALITY REPORT

21%	18%	19%	9%
SIMILARITY INDEX	INTERNET SOURCES	PUBLICATIONS	STUDENT PAPERS

PRIMARY SOURCES

1	St Sabahannur, Suraedah Alimuddin, St Subaedah, Nurul Wahdaniya, Firda Yunita Faharuddin. "The Effect of Cocoa Butter Substitute (CBS) Produced from Palm Kernel Oil and Virgin Coconut Oil (VCO) on The Quality of Milk Chocolate", Research Square Platform LLC, 2023 Publication	3%
2	ouci.dntb.gov.ua Internet Source	3%
3	repository.petra.ac.id Internet Source	2%
4	iwaponline.com Internet Source	2%
5	Shi-Lan Su, Jing-Hua Xiao, Wei-Qing Liu, Ye Wu. "Synchronization mechanism of clapping rhythms in mutual interacting individuals*", Chinese Physics B, 2021 Publication	1%
6	www.mdpi.com Internet Source	1%

7	Mohamed Shaban, Mostafa R. Abukhadra, Suzan S. Ibrahim, Mohamed .G. Shahien. "Photocatalytic degradation and photo-Fenton oxidation of Congo red dye pollutants in water using natural chromite—response surface optimization", Applied Water Science, 2017 Publication	1 %
8	www.jeeng.net Internet Source	1 %
9	F Riyanti, P L Hariani, Fatma, N Yuliasari, M Said, T Ramadiati. " Synthesis of chitosan-SiO composite for adsorption methyl dyes from solution ", IOP Conference Series: Materials Science and Engineering, 2020 Publication	1 %
10	M. Keerthana, Mayuri Ingle, T. Pushpa Malini, R. Sangavi. "VISIBLE LIGHT ASSISTED PHOTOCATALYTIC DEGRADATION OF CARCINOGENIC CONGO RED DYE USING GREEN SYNTHESIZED YTTRIUM AND ZINC DOPED NICKEL OXIDE NANOPARTICLES FROM CORIANDER LEAF EXTRACT", RASAYAN Journal of Chemistry, 2022 Publication	1 %
11	Submitted to Universitas Diponegoro Student Paper	1 %

12	journal.gnest.org Internet Source	1 %
13	link.springer.com Internet Source	1 %
14	ijtech.eng.ui.ac.id Internet Source	1 %
15	Hicham Meskher, Fethi Achi, Fatah Ben Moussa, Abdellah Henni, Hakim Belkhelfa. "A Novel Pentachlorophenol Electrochemical Sensor Based on Nickel-Cobalt Layered Double Hydroxide Doped with Reduced Graphene Oxide Composite", ECS Advances, 2023 Publication	1 %
16	Monir-Sadat Shakeri. "Antimicrobial activity of Zataria multiflora Boiss. essential oil incorporated with whey protein based films on pathogenic and probiotic bacteria : Antimicrobial activity of Zataria multiflora", International Journal of Food Science & Technology, 03/2011 Publication	1 %
17	www.oak.go.kr Internet Source	1 %
18	Fahmideh Shabani, Ali Khodayari. " Structural, Compositional, and Biological	1 %

Characterization of Fe O Nanoparticles Synthesized by Hydrothermal Method ", Synthesis and Reactivity in Inorganic, Metal-Organic, and Nano-Metal Chemistry, 2014
Publication

19 Submitted to Rutgers University, New Brunswick
Student Paper

1 %

Exclude quotes	On	Exclude matches	< 1%
Exclude bibliography	On		